International Journal of Electrical Engineering.
ISSN 0974-2158 Volume 15, Number 1 (2022), pp. 21-43

http://www.irphouse.com

An Effective Adaptive Sliding Mode Control Strategy for Power Optimization in Standalone Solar Photovoltaic System

Anbarasi MP[1], S Kanthalakshmi[2], V Easwaran[3]

[1, 2,3] PSG College of Technology, Coimbatore, India.

Abstract

This paper proposes an adaptive sliding mode control strategy for power optimization in solar photovoltaic system. The objective is to operate the photovoltaic system at its maximum power point irrespective of changes in environmental conditions and in this paper the objective is met by designing the maximum power point tracking controller based on adaptive sliding mode control algorithm. The photovoltaic system chosen is the stand-alone PV module which is modeled using first principle approach. The sliding surface is designed to reach maximum power point based on incremental conductance method. The performance of adaptive sliding mode controller is proven to be better than sliding mode controller, by comparing the oscillations and speed of tracking of the photovoltaic module power.

Keywords: Adaptive control, Sliding mode control (SMC), DC-DC Power converter, Maximum power point tracker (MPPT), Solar Photovoltaics.

I. INTRODUCTION

Each year the demand for oil and gas is increasing significantly and so, energy security is a major concern worldwide (Leon and David 2008). Globally, the energy potential of coal, oil, gas and uranium are, by and large, confined to a few geographically limited sites. A close look at the potential of primary energy sources like wind, biomass, and hydro reveals that though these resources are distributed much more widely, their techno-economic utility is still limited due to geographical constraints. In contrast, solar energy happens to be the sole primary energy source that can be directly exploited at any point on the earth (Suneel 2011). Apart from its abundant availability, solar energy is a good option and the electricity produced is clean, long lasting, non-radioactive and pollution free (Enrico et al. 2013). It has experienced a remarkable growth for the past two decades in its widespread use from

standalone to utility interactive PV systems. All these factors make solar energy attractive (Suneel 2011). There are many ways of extracting solar energy, one such method is using the photovoltaic effect that consists of a direct transformation of sunlight into electricity by means of solar panels (Tamal, Panda and Saha 2013). Even though the PV system is posed to its high capital fabrication cost and low conversion efficiency, the skyrocketing oil prices make solar energy naturally viable energy supply with potentially long-term benefits.

The appliances like computers, LED lights, cell phones and so on use their own rectifiers to switch power from AC to DC. The photovoltaic technology is well poised to be integrated with majority of these applications and much more efficient solution would be to install solar PV system that operates at its maximum potential (Lyden and Haque, 2015). Also, as the PV system's initial installment cost is also high, it is essential that the PV system should be operated to extract maximum possible power throughout the year and this increases the return for investment (Zahra, Saad and Mohsen 2013). To increase the electrical efficiency, lot of efforts is made, often forgetting that the total efficiency is the product of electrical efficiency by the maximum power point tracking (MPPT) efficiency (Yoash and Doron 2013). So, to improve the efficiency of the PV system, maximum power has to be extracted from it and this can be done by either adjusting the load connected to it or by implementing the MPPT algorithm. As adjusting the load is not a better control mechanism, MPPT algorithm is implemented and its design for the PV system is an important process. The MPPT is an online algorithm which dynamically changes the operating point of the solar panels (Saravanan and Ramesh 2016; Amevi and Essel 2013). The main hindrance in operating the PV system efficiently is existence of non-uniform environmental conditions. The maximum power point (MPP) will vary due to the rapidly changing external environmental conditions like temperature, dirt, shadow, irradiation and so on (Kumaresh et al. 2014). In short, the maximum power from the PV module varies according to the outdoor environment where it is installed. The above factors create the necessity for MPPT techniques.

There are many MPPT techniques available and commonly used methods are Perturb and Observe (P&O), Incremental Conductance (INC), Fractional short-circuit current, Fractional open-circuit voltage, Sliding Mode Control, Fuzzy based controllers, and so on (Alsumiri, Jiang, Tang 2014). Each of the methods has their own advantages and disadvantages, which are reviewed in several MPPT literatures (Hamid 2016). Recently adaptive controllers are also included while designing the MPPT techniques. Most of the MPPT algorithms uses switching converters to extract and transfer the maximum power to the load. As the PV system is a nonlinear system, nonlinear MPPT control techniques are very useful to operate the PV module at its MPP (Meenal and Nilanshu 2013).

In this paper, typical nonlinear control approach, adaptive sliding mode controller is applied, which exploits the inherent variable structure nature of switching converter. The systems whose physical structures changes with respective to control law are said to have variable structure nature (Tamal, Panda and Saha 2013). The adaptive sliding mode controller (ASMC) is developed from sliding mode controller (SMC), which

incorporates the advantages of SMC. The SMC has the advantages such as insensitivity to system parameter changes, disturbance and load variations. It is also a robust controller (Maissa, Oscar and Lassad 2016). But the major disadvantage in SMC is chattering phenomenon. It becomes inevitable to have a controller which minimizes the chattering phenomenon and also compensates the PV model uncertainties that occur due to the changes in environmental conditions. So ASMC is proposed and compared with SMC. The comparison is made to prove that the ASMC will perform better than SMC. This paper is organized as follows; the PV system modeling is given in section II. The section III deals with the MPPT concept. The proposed ASMC for MPPT is discussed in section IV. The simulation results are given in section V. Also, comparative analysis between SMC and ASMC is performed in this section. Section VI comprises of conclusion.

II. PV SYSTEM MODELING

The chosen PV module can provide an output of 37.11 W at ambient temperature of 25℃ and irradiation of 1000 W/m^2. The module is connected to load through DC-to-DC boost converter. The DC-to-DC boost converter is used to transfer the maximum extracted power from the PV module to the stand-alone load. Also, to obtain load voltage greater than module output voltage boost converter is selected (Daniel, Carloss and Roberto 2016). The duty ratio of the converter is controlled through ASMC accounting for changes in irradiation and temperature. The overall block diagram of the system is given in the Fig. 1.

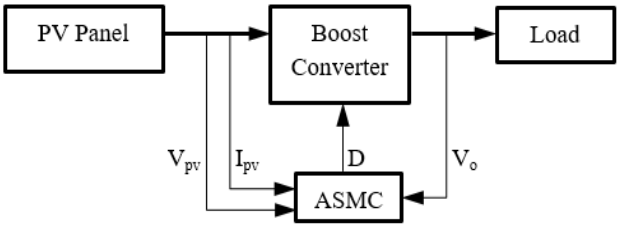

Fig. 1. Overall block diagram of the PV system.

The ASMC uses the PV module voltage (V_{pv}), PVmodule current (I_{pv}) and load voltage (V_o) to generate duty ratio (D) in order to extract maximum power.

A. Mathematical Model of PV Module

A PV module is a series and parallel combinations of solar cells connected together to obtain the desired current and voltage from the panel (Enrico et al. 2013). The typical PV module is shown in the below figure 2.

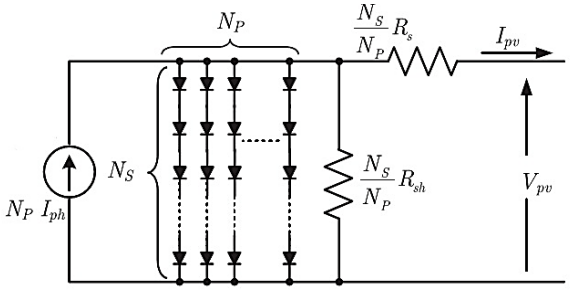

Fig. 2. Equivalent circuit of PV module.

The single-diode model is primarily used to model a PV cell, which offers good trade-off between simplicity and accuracy. The mathematical representation of the entire PV module is derived from the basic physical laws of semiconductors. The basic equations from the theory of semiconductors and photovoltaics are used and are listed below (Chetan Singh Solanki 2011).

$$I_{pv} = N_p I_{ph} - N_p I_s [e^{\frac{q(V_{pv}+I_{pv}R_s)}{N_s AKT}} - 1] \quad (1)$$

$$I_{ph} = [I_{scr} + K_i(T - T_{ref})]\frac{\lambda}{1000} \quad (2)$$

$$I_s = I_{rs}\left(\frac{T}{T_{ref}}\right)^3 e^{\frac{qEgo}{AK}\left[\frac{1}{T_{ref}} - \frac{1}{T}\right]} \quad (3)$$

$$I_{rs} = \frac{I_{scr}}{e^{\frac{q(V_{OC})}{N_s AKT}} - 1} \quad (4)$$

Where,

I_{pv}- Module output current (A)

V_{pv}- Module output voltage (V)

I_{ph} - Module photocurrent (A)

I_s - Module saturation current (A)

I_{rs} - Module reverse saturation current (A)

I_{scr} - Module short circuit current (A)

K_i - Temperature coefficient (0.0017 A/K)

T - Actual temperature (K)

T_{ref} - Reference temperature (K)

λ- Irradiation on the device surface (w/m^2)

q - Electron charge (1.6 x 10^{-19} C)

V_{oc} - Open circuit voltage(V)

N_s - No. of cells connected in series

K - Boltzmann constant (1.3805 x 10^{-23} J/K)

A - Ideality factor

N_p- No. of parallel cells in the module

R_s- Equivalent series resistance (Ω)

The electrical characteristic data of chosen 37.11 W solar module are listed in Table I.

TABLE I. Electrical Characteristic Data of the Chosen PV Module

Description	Rating
Rated Power	37.11 W
Voltage at maximum power (V_{mp})	16.56 V
Current at maximum power (I_{mp})	2.25 A
Open circuit voltage (V_{oc})	21.24 V
Short circuit current (I_{scr})	2.55 A
Total no.of cells in series (N_s)	36
Total no.of cells in parallel (N_p)	1

The electrical characteristics of37.11W PV module at 25℃ for various irradiations are shown in the Fig.3 and Fig.4. Similarly, the electrical characteristics at 1000 W/$m^2$for various temperatures are shown in the figures Fig.5 and Fig.6.

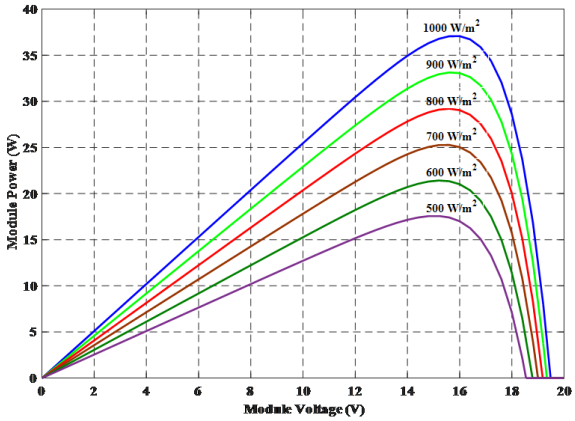

Fig. 3. P-V characteristic of PV module with constant temperature.

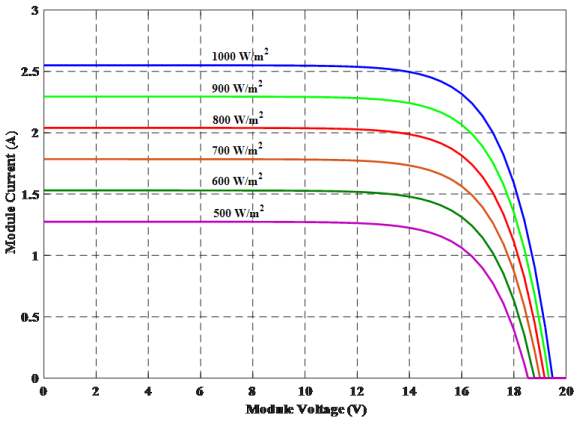

Fig. 4. I-V characteristic of PV module with constant temperature.

The effect of solar irradiation is analyzed through figures 3 and 4. The module power (P_{pv}) strongly depends on the irradiation falling on it. The P_{pv} decreases linearly with the decrease in intensity of solar radiation. So, throughout the day due to the variation in the irradiation, P_{pv} also varies. The module current is the linear function of irradiation. Thus, if the radiation is half the peak radiation intensity, the module will produce half the peak current (Chetan Singh Solanki 2011).

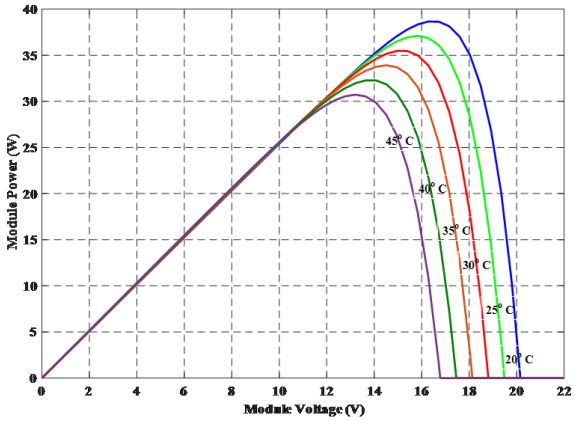

Fig. 5. P-V characteristic of PV module with constant irradiation.

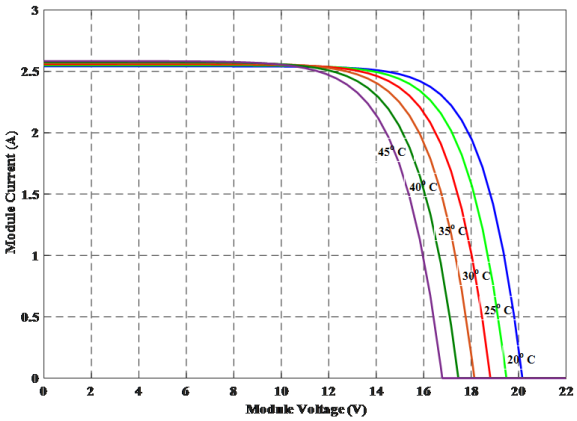

Fig. 6. I-V characteristic of PV module with constant irradiation.

The figures Fig. 5 and Fig. 6 shows that P_{pv} also depend on the temperature at which the module is operating. The variation in actual module temperature (*T*) depends on the conditions such as radiation intensity, wind speed, etc. The increase in temperature results in an increase in the short circuit current I_{scr} and decrease in the open circuit voltageV_{oc}. Decrease in V_{oc} is more prominent than the increase in theI_{scr} (Chetan Singh Solanki 2011). Therefore, overall, the power output and efficiency of PV module decrease with the increase in its operating temperature. Finally, it is evident that the irradiation and temperature are the two important factors, which affect the characteristics of the PV module.

B. DC to DC Boost Converter

The converters come under category – balance of solar PV systems. Among the different types of converters, the boost converter is chosen due to the various reasons

stated in various literatures (Lachtar et al. 2019). A boost converter is a DC-to-DC converter that provides an output voltage greater than the source voltage depending on changes in the duty ratio (D). The variation in duty ratio can be used not only to regulate load voltage (V_o) but also to vary the input side impedance (R_{in}) of the converter. This helps in the application of MPPT in PV modules. The boost converter can be controlled to present optimum impedance across the PV module terminals which facilitate maximum power extraction from the module. This feature can be appreciated by inspecting the following expression of R_{in}.

$$R_{in} = R(1 - D)^2 \tag{5}$$

$$D = 1 - \frac{V_{pv}}{V_o} \tag{6}$$

As the value of D can vary between 0 and 1, the input impedance seen at the input side of the boost converter also varies and it will be always less than the load impedance. The model of boost converter's dynamic behavior is needed to design MPPT controller. Figure 7 shows the configuration of boost converter used in this paper. It has inductor (L), MOSFET (SW), diode (D_i) and capacitor (C).

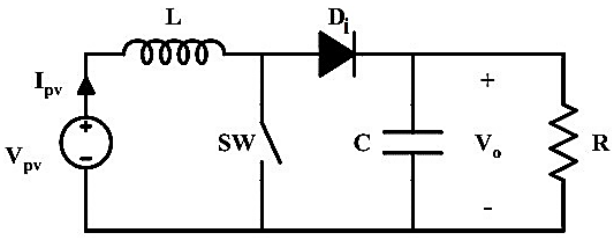

Fig. 7. Configuration of DC-to-DC boost converter.

The state space equations of boost converter are obtained through state space averaging method and are given in the equations 7 and 8. The state space model is represented through the equation 9.

$$\frac{dI_{pv}}{dt} = \frac{V_{pv}}{L} - \frac{(1-D)V_o}{L} \tag{7}$$

$$\frac{dV_o}{dt} = \frac{(1-D)I_{pv}}{L} - \frac{V_o}{RC} \tag{8}$$

$$\begin{bmatrix} \dot{I_{pv}} \\ \dot{V_o} \end{bmatrix} = \begin{bmatrix} 0 & -\frac{(1-D)}{L} \\ \frac{(1-D)}{L} & -\frac{1}{RC} \end{bmatrix} \begin{bmatrix} I_{pv} \\ V_o \end{bmatrix} + \begin{bmatrix} \frac{1}{L} \\ 0 \end{bmatrix} V_{pv} \tag{9}$$

The equation 7 is later used to design the control law for SMC. The specifications of boost converter are listed in Table II.

TABLE II. Specifications of Selected Boost Converter

Parameters	Rating
Inductance (L)	290 µH
Capacitance (C)	330 µF
Switch frequency (f_{SW})	10 KHz
Load resistance (R)	50 Ω

III. MAXIMUM POWER POINT TRACKING

From the detailed discussions made in the introduction part, it is clearly observed that the MPPT system is one of the essential parts of the any PV system and will certainly result in improving the efficiency of the PV system. The operating point of the solar PV module is decided by the load connected to it. Due to the environmental changes, this operating point changes throughout the day. But maximum power has to be transferred to load under all operating conditions. So, to ensure the operation of PV module for maximum power transfer, a special method called MPPT is employed in PV systems (Huan, Ci and Yi 2008).

The MPPT mechanism is based on the principle of impedance matching between load and PV module. To achieve this principle, MPPT makes use of an algorithm called as MPPT algorithm and an electronic circuitry, which will mostly be a converter circuit (Chetan Singh Solanki 2011). As discussed in section II, DC to DC boost converter is used for impedance matching. The P-V characteristics show that the maximum power changes with the changes in irradiation and temperature respectively. And it can also be understood that the maximum power can be tracked by operating the PV module at a particular module voltage for a particular irradiation or for a particular temperature. So there is a dependency of maximum power on the module voltage V_{pv}.

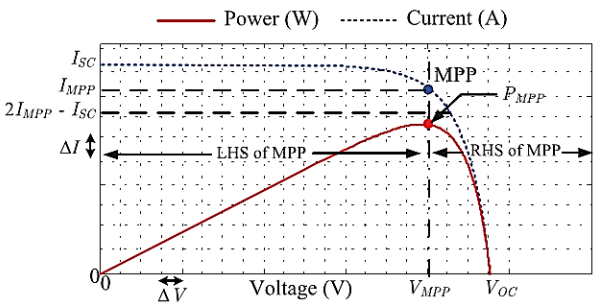

Fig. 8. Operating characteristics of PV module.

The MPP concept is illustrated in figure 8, where the maximum power P_{MPP} is obtained at MPP voltage (V_{MPP}). Mostly, this principle of MPPT is based on adaptive or varying converter duty ratio to finally bring the operating point to MPP. TheV_{pv}, I_{pv} and $V_o$are measured and used as inputs to the algorithm which then adjusts the duty ratio (D) of the converter, resulting in the adjustment of the reflected load impedance (R_{in}). Now the MPPT problem can be defined as the designing of a controller that allows tracking of MPP by controlling appropriateV_{MPP}, despite the variations in temperature or solar irradiation (Hamid 2016).

The algorithms like Perturb and Observe, Incremental Conductance, Fractional short-circuit current and Fractional open-circuit voltage controls the duty cycle to reach MPP. The SMC is one such controller which adjusts the duty cycle and forces the operating point (MPP) to lie in a point at the top of the curve where the condition of maximum power is achieved. However, SMC has major drawback of chattering and it should be tuned for modeling errors, external disturbance and model parameter variations that occurs due to changing environmental condition. Optimizing the sliding mode controller's parameters or fine tuning them for these variations is complex one. Another way to resolve this controller parameter issue is to design a SMC that adapt itself to the modeling uncertainties and environmental changes with minimum chattering. Hence adaptive sliding mode controller is proposed and designed, wherein the controller parameter of SMC is adapted depending on the changes in the irradiation and temperature.

IV. PROPOSED ADAPTIVE SLIDING MODE CONTROLLER FOR MPPT

The SMC derived from variable structure system theory, extends the properties of hysteresis control to multivariable environments. It gives good dynamic response and is simpler for implementation (Christopher and Sarah, 2008). The SMC is applied to the boost converter. The converter switches depend on the instantaneous values of state variables of the boost converter to force the system trajectory to stay on a suitable surface on the phase plane. The design of SMC is based on equivalent control method and the method involves two steps, in first step sliding surface is designed and in second step the discontinuous control is designed. Here the sliding surface is designed based on incremental conductance (INC) method (Zahra, Saad and Mohsen 2013).

A. Incremental Conductance Method

The INC method's baseline is that the slope of the PV module power curve is zero at the MPP, positive when the operating point is on the left of MPP and negative when the operative point is on the right of MPP. In this method PV power is differentiated with respective to PV voltage and this value will be zero at MPP. The above concept can be expressed as:

$$\frac{dP_{pv}}{dV_{pv}} = \frac{d(V_{pv}I_{pv})}{dV_{pv}} = I_{pv} + V_{pv}\frac{dI_{pv}}{dV_{pv}} = I_{pv} + V_{pv}\frac{\Delta I_{pv}}{\Delta V_{pv}} \quad (10)$$

The equation 10 will be zero at MPP, positive on left of MPP and negative on the right of MPP. The controller is forced to operate at reference voltage (V_{ref})to attain MPP. The 'V_{ref}' is either incremented or decremented by following the given algorithm to operate the PV system at MPP [9], [11].

1. Read $V_{pv}(t)$ and $I_{pv}(t)$.
2. Calculate ΔI_{pv} and ΔV_{pv} as follows,

$$\Delta I_{pv} = I_{pv}(t) - I_{pv}(t - \Delta t) \quad (11)$$

$$\Delta V_{pv} = V_{pv}(t) - V_{pv}(t - \Delta t) \quad (12)$$

3. Check for$\Delta V_{pv} = 0$. If the condition is true, then go to step 8 or else go to step 4.
4. Check the condition$(\Delta I_{pv}/\Delta V_{pv}) = -(I_{pv}/V_{pv})$. If true, then go to step 10 or else go to step 5.
5. Check the condition$(\Delta I_{pv}/\Delta V_{pv}) > -(I_{pv}/V_{pv})$. If true, then go to step 7 or else go to step 6.
6. Decrement V_{ref} and go to step 10.
7. Increment V_{ref} and go to step 10.
8. Check for$\Delta I_{pv} = 0$. If the condition is true, then go to step 10 or else go to step 9.
9. Check for$\Delta I_{pv} > 0$. If the condition is true, then go to step 7 or else go to step 6.
10. Update $I_{pv}(t - \Delta t)$ and $V_{pv}(t - \Delta t)$.

$$I_{pv}(t - \Delta t) = I_{pv}(t) \quad (13)$$

$$V_{pv}(t - \Delta t) = V_{pv}(t) \quad (14)$$

11. Return to step 1 for new measurements.

B. Sliding Mode Controller Design

The sliding surface (σ) is chosen as the error between Instantaneous resistance ($R_i = V_{pv}/I_{pv}$) and Incremental resistance ($r_i = |dV_{pv}/dI_{pv}|$). These conditions will result in the following equations.

$$\sigma = R_i - r_i \quad (15)$$

The structure of the control law$u(t)$ is defined as sum of equivalent control input $u_{eq}(t)$ and nonlinear switching input$u_n(t)$ [13], [24]. So, control law is given as,

$$u(t) = u_{eq}(t) + u_n(t) \quad (16)$$

The equivalent control input defines the system's behavior on the sliding surface and it is determined using invariance condition as stated in equation (17).

$$\dot{\sigma} = 0 \quad (17)$$

At this condition the controller effort will be $u_{eq}(t)$ and since the controller effort is the duty ratio of boost converter, $u_{eq}(t)$ will beequal to D. Now from equations (7), (15) and (17), following equation for $u_{eq}(t)$ is derived.

$$u_{eq}(t) = 1 - \frac{V_{pv}}{V_o} \quad (18)$$

The nonlinear switching input moves the state to the sliding surface and keeps the state on the sliding surface in the presence of uncertainty. This is chosen such that the Lyapunov stability criterion is met. Equation (19) states Lyapunov stability criteria.

$$d\sigma . \sigma < 0 \quad (19)$$

The chosen nonlinear switching input is given in equation (20) and controller parameter M is derived later.

$$u_n(t) = \frac{V_{pv}}{V_o} - M \quad (20)$$

From equations (16), (18) and (20) the control law is derived as:

$$u(t) = 1 - M \quad (21)$$

A Lyapunov function and its time derivative are defined as:

$$V = \frac{\sigma^2}{2} \tag{22}$$

$$dV = \sigma . d\sigma \tag{23}$$

From equations (7), (15), (21) and (23), the following equation is obtained.

$$dV = \left(\frac{\partial R_i}{\partial I_{pv}} - \frac{\partial r_i}{\partial I_{pv}}\right)(V_{pv} - MV_o)\frac{\sigma}{L} \tag{24}$$

The INC method proves that $\left(\frac{\partial R_i}{\partial I_{pv}} - \frac{\partial r_i}{\partial I_{pv}}\right)$ part in (24) is always negative.

$$\left(\frac{\partial R}{\partial I_{pv}} - \frac{\partial r}{\partial I_{pv}}\right) < 0 \tag{25}$$

Based on equation (15) for$\sigma < 0$,

$$\frac{V_{pv}}{I_{pv}} < \left|\frac{dV_{pv}}{dI_{pv}}\right|$$

For any positive parameter ‘α’,

$$\left(\frac{V_{pv}}{I_{pv}}\right)^{\alpha} < \left(\left|\frac{dV_{pv}}{dI_{pv}}\right|\right)^{\alpha} \tag{26}$$

Multiply the above inequality (26) with the following expression (27) to obtain the equation (28).

$$\frac{(V_{pv})^{(1-\alpha)}(I_{pv})^{\alpha}}{V_o} > 0 \tag{27}$$

So, for $\sigma < 0$,

$$\frac{V_{pv}}{V_o} < \frac{(V_{pv})^{(1-\alpha)}(I_{pv})^{\alpha}}{V_o}\left(\left|\frac{dV_{pv}}{dI_{pv}}\right|\right)^{\alpha} \tag{28}$$

Similarlyfor$\sigma > 0$,

$$\frac{V_{pv}}{V_o} > \frac{(V_{pv})^{(1-\alpha)}(I_{pv})^{\alpha}}{V_o}\left(\left|\frac{dV_{pv}}{dI_{pv}}\right|\right)^{\alpha} \quad (29)$$

Based on (28) and (29), it can be said that variable structure exists through the ratioV_{pv}/V_o. The M in control law can be chosen as:

$$M = \frac{(V_{pv})^{(1-\alpha)}(I_{pv})^{\alpha}}{V_o}\left(\left|\frac{dV_{pv}}{dI_{pv}}\right|\right)^{\alpha} \quad (30)$$

In order to prove the lyapunov stability criteria consider the followings:

For$\sigma < 0$, based on (28) and (30)

$$V_{pv} - MV_o < 0$$

So,$\sigma(V_{pv} - MV_o) > 0$ (31)

For$\sigma > 0$, based on (29) and (30)

$$V_{pv} - MV_o > 0$$

So, $\sigma(V_{pv} - MV_o) > 0$ (32)

From equations (24), (25), (31) and (32), it is proved that the time derivative of chosen Lyapunov function is negative. Based on equations (21) and (30) the final control law will be,

$$u(t) = 1 - \frac{(V_{pv})^{(1-\alpha)}(I_{pv})^{\alpha}}{V_o}\left(\left|\frac{dV_{pv}}{dI_{pv}}\right|\right)^{\alpha} \quad (33)$$

After designing the control law for SMC, the adaptive sliding mode controller is designed by adapting the sliding mode controller's parameter to the changes in the

irradiation and temperature. The controller parameter 'α' is adapted as,

$$\alpha = \frac{V_{pv}}{V_o} \qquad (34)$$

But the duty ratio D lie between 0 and 1, so the real control signal will be,

$$D = \begin{cases} 0, & u(t) \leq 0 \\ u(t), & 0 < u(t) < 1 \\ 1, & u(t) \geq 1 \end{cases} \qquad (35)$$

V. SIMULATION RESULTS

The block diagram shown in Fig. 1 is modeled and simulated in MATLAB/Simulink. The simulation is done for both SMC and ASMC by varying the irradiation and temperature. The PV module specifications are shown in Table I. The PV module power for irradiation of 1000 W/m^2 and for temperature of 25℃with SMC and ASMC are shown in Fig. 9 and Fig. 10 respectively. The Fig. 11, Fig. 12 and Fig.13 show the variations in PV module power, voltage and current with change in irradiation from 500 W/m^2 to 1000 W/m^{2}at 25℃ while using SMC respectively and Fig. 14, Fig. 15 and Fig. 16 show the variations in PV module power, voltage and current with change in irradiation from 500 W/m^2 to 1000 W/m^2 at 25℃ while using ASMC respectively.

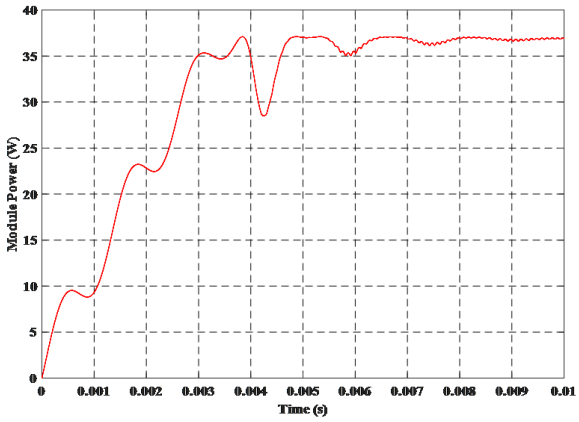

Fig. 9. PV module power for constant irradiation of 1000 W/m^{2}at25℃with SMC.

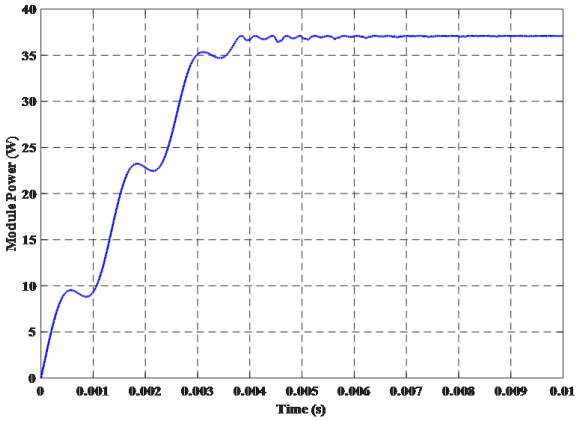

Fig. 10. PV module power for constant irradiation of 1000 W/m^2 at 25℃with ASMC.

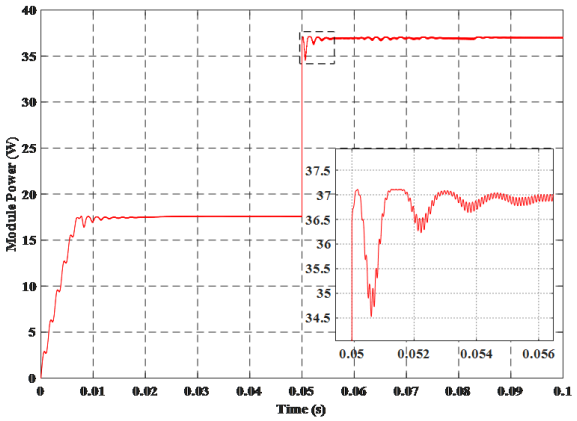

Fig. 11. PV module power for change in irradiation from 500 W/m^2 to 1000 W/m^2 at 25℃with SMC.

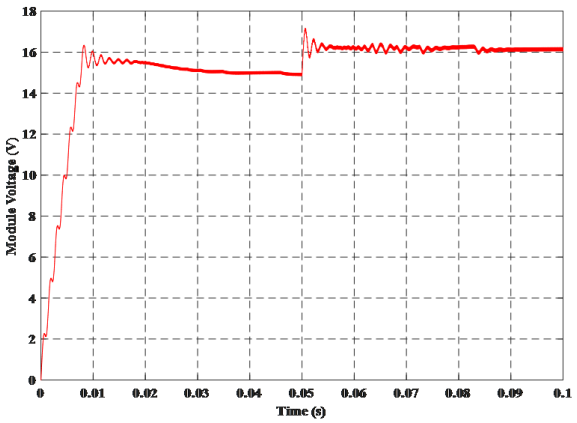

Fig. 12. PV module voltage for change in irradiation from 500 W/m^2 to 1000 W/m^2 at 25℃with SMC.

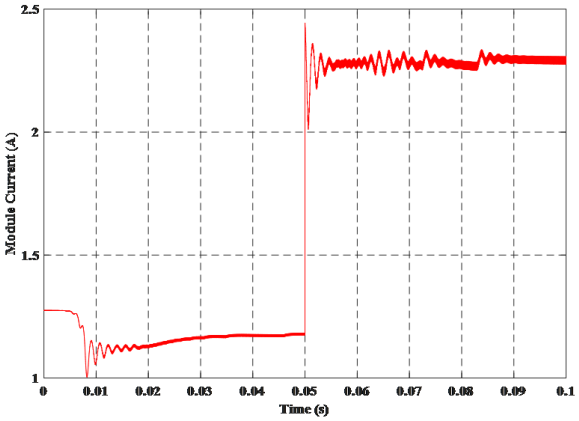

Fig. 13. PV module current for change in irradiation from 500 W/m^2 to 1000 W/m^2 at 25℃ with SMC.

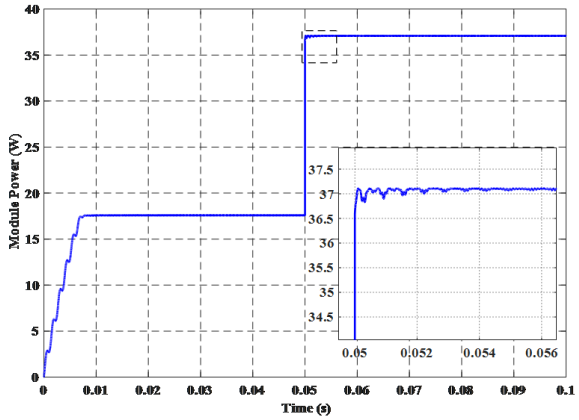

Fig. 14. PV module power for change in irradiation from 500 W/m^2 to 1000 W/m^2 at 25℃ with ASMC.

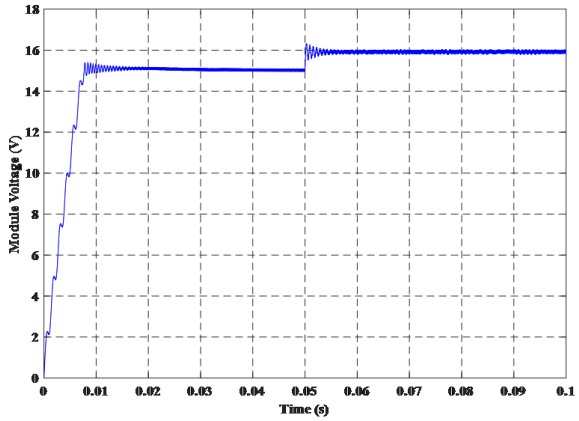

Fig. 15. PV module voltage for change in irradiation from 500 W/m^2 to 1000 W/m^2 at 25℃ with ASMC.

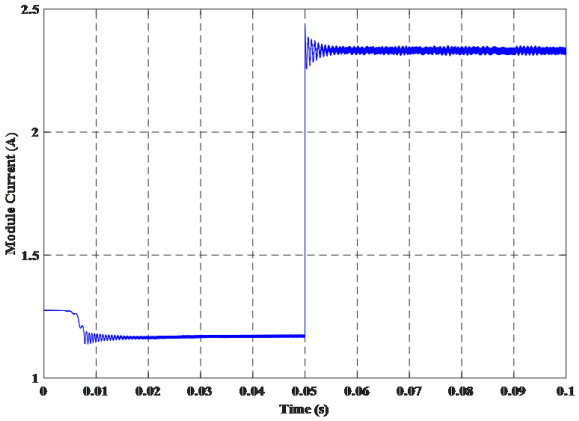

Fig. 16. PV module current for change in irradiation from 500 W/m^2 to 1000 W/m^2 at 25℃ with ASMC.

TABLE III. Variations in PV Module Power, Voltage and Current

λ(w/m^2)	T (℃)	Desired P_{pv} (W)	Simulated values			Settling time (ms)
			P_{pv} (W)	V_{pv} (V)	I_{pv} (A)	
1000	25	37.11	37.1	15.8	2.32	5.1
	35	33.92	33.9	14.6	2.32	3.5
800	25	29.2	29.2	15.65	1.85	4.2
	35	26.59	26.63	14.35	1.85	4.9

The Table III indicates the simulated values, desired module power and tracking speed for various irradiation and temperature changes with adaptive sliding mode controller. Fig. 17, Fig.18 and Fig. 19 shows the variations in PV module power, voltage and current with change in temperature from 25℃ to 35℃ at 1000 W/m^2 while using SMC respectively.

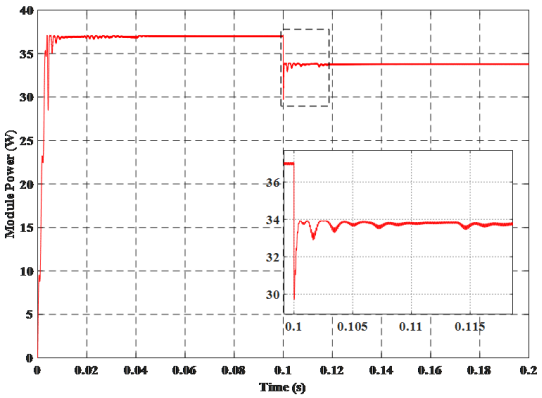

Fig. 17. PV module power for change in temperature from 25℃ to 35℃ at 1000 W/m^2 with SMC.

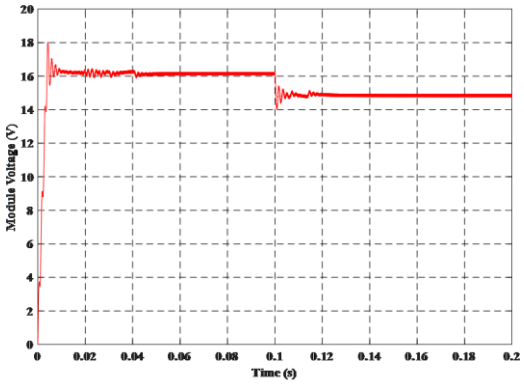

Fig. 18. PV module voltage for change in temperature from 25℃ to 35℃ at 1000 W/m^2 with SMC.

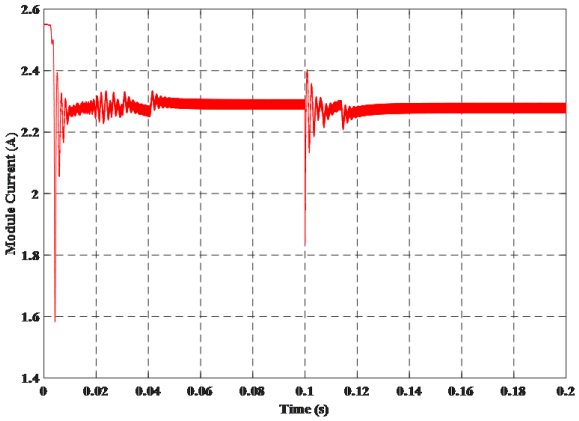

Fig. 19. PV module current for change in temperature from 25℃ to 35℃ at 1000 W/m^2 with SMC.

Fig. 20, Fig. 21 and Fig. 22 shows respectively the variations in PV module power, voltage and current with change in temperature from 25°C to 35°C at 1000 W/m^2 while using ASMC.

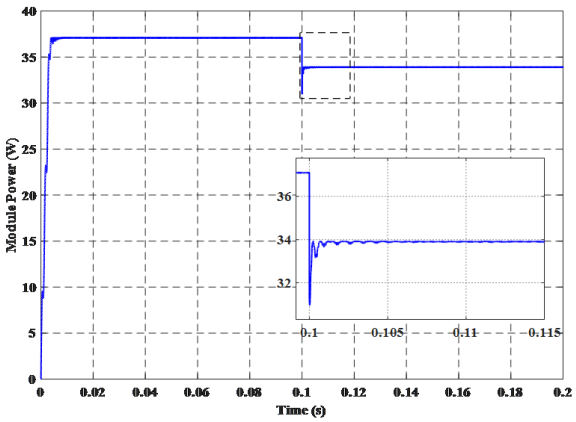

Fig. 20. PV module power for change in temperature from 25°C to 35°C at 1000 W/m^2 with ASMC.

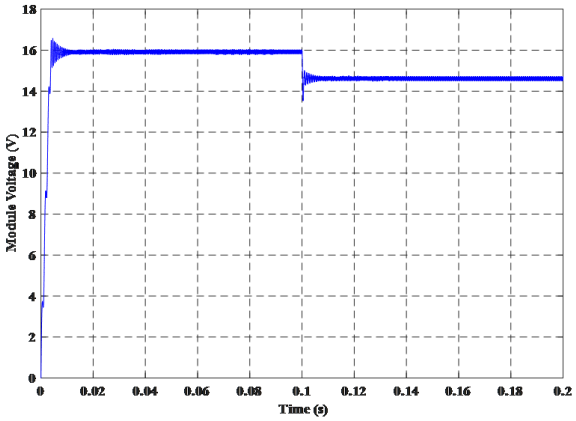

Fig. 21. PV module voltage for change in temperature from 25°C to 35°C at 1000 W/m^2 with ASMC.

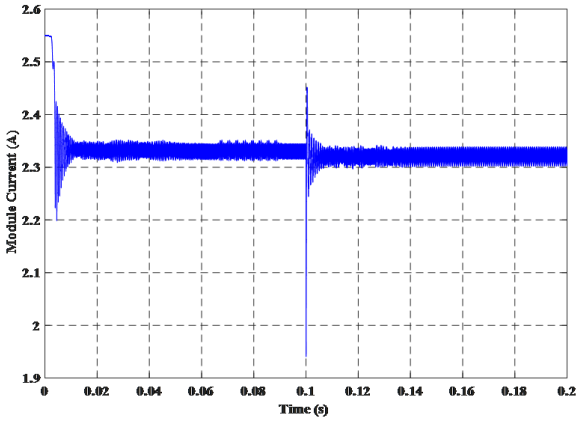

Fig. 22. PV module current for change in temperature from 25℃ to 35℃ at 1000 W/m^2 with ASMC.

The simulations are carried out for the irradiations 1000 W/m^2 and 800W/m^2 with temperatures 25℃ and 35℃. From Fig. 9 and Fig. 10, it can be inferred that the ASMC tracks the maximum power faster than SMC and it also improves the stability by reducing the oscillations present in PV module power. From Table III, it is proved that the proposed ASMC forces the operating point of the PV module to lie on the maximum power point irrespective of changes in irradiation and temperature. The settling time also fast enough with minimum chattering effect. Thus, ASMC provides faster dynamics. Fig 11 to Fig. 16 shows that the settling speed of PV module's output parameters with ASMC are faster, when there is change in irradiation. On the other hand, SMC gives more oscillatory results. Similarly, the figures from Fig. 17 to Fig. 22 also prove that ASMC provides better response than the SMC. Also, the tracking speed of ASMC is faster than SMC when there is a change in temperature. Ultimately, the proposed adaptive sliding mode controller exhibits better performance, when compared to SMC.

VI. CONCLUSION

The maximum power has been extracted from solar PV module by the proposed ASMC and transferred to the load through DC-to-DC boost converter. To analyse the performance of ASMC for MPPT in PV module, the closed loop PV system with ASMC is designed and simulated. The PV module is modeled using first principle approach and its output power variation for various irradiations is recorded. Then to obtain maximum power from PV module, SMC with the objective of MPPT is designed. The MPPT is achieved by varying the impedance of PV through boost converter. To improve the tracking speed and to minimize the oscillations in the PV output electrical parameters, the control parameter of SMC is adapted to the changes in the irradiations. Thus, the PV system with ASMC is simulated and proved that the

ASMC gives better result when compared with SMC. It is also noted that ASMC gives superior transient and steady state responses than SMC.

REFERENCES

[1] Alsumiri, M.A., L. Jiang, and W.H. Tang. 2014. "Maximum power point tracking controller for photovoltaic system using sliding mode control," *IET. Renewable Power Generation Conference* 1–5.

[2] AmeviAcakpovi, and Essel Ben Hagan. 2013. "Novel photovoltaic module modeling using matlab/simulink." *International Journal of Computer Applications 83(16):* 27–32.

[3] Chetan Singh Solanki. 2011. "*Solar Photovoltaics – Fundamentals, Technologies and Application.,* 2nd ed. New Delhi: PHI Learning Private Limited *337–381.*

[4] Christopher Edwards and Sarah K. 1998. "*,SlidingModeControl: Theory and Applications."* USA: CRC Press.

[5] Daniel Gonzalez Montoya, Carlos Andres Ramos Paja, and Roberto Giral. 2016. "Maximum power point tracking of photovoltaic systems based on the sliding mode control of the module admittance." *Electric Power Systems Research*, 136: 125–134.

[6] Daniel Gonzalez Montoya, Carlos Andres Ramos-Paja, and Roberto Girali. 2016. "Improved design of sliding-mode controllers based on the requirements of MPPT techniques." *IEEE Trans. Power Electronics*, 31(1): 235–247.

[7] Enrico Bianconi, Javier Calvente, Roberto Giral, Emilio Mamarelis, Giovanni Petrone, Carlos Andrés Ramos-Paja, Giovanni Spagnuolo, and Massimo Vitelli. 2013. "A fast current-based MPPT technique employing sliding mode control." *IEEE Trans. Industrial Electronics*, 60(3): 1168–1178.

[8] Ghazanfari, J., and M. M. Farsangi. 2013. "Maximum power point tracking using sliding mode control for photovoltaic array," *Iranian Journal of Electrical & Electronic Engineering 9(3):* 189–196.

[9] Hamid Reza Koofigar. 2016. "Adaptive robust maximum power point tracking control for perturbed photovoltaic systems with output voltage estimation," *ISA Transactions* 60: 285–293.

[10] Huan-Liang Tsai, Ci-Siang Tu, and Yi-JieSu. 2008. "Development of generalized photovoltaic model using MATLAB/SIMULINK." in *Proc. World Congress on Engineering and Computer Science,* San Francisco, USA.

[11] Kumaresh, V., Mridul Malhotra, Ramakrishna, N., and Saravana Prabu.R. 2014. Literature review on solar MPPT systems. *Advance in Electronic and Electric Engineering. 4(3):* 285–296.

[12] Lachtar, S., Bouraiou, B., Diaafri, O., and Maouedj, R. 2019. "Smooth Sliding

Mode-Based MPPT Algorithm for Photovoltaic Applications," 2019 1st Global Power, Energy and Communication Conference (GPECOM) 253-258, doi: 10.1109/GPECOM.2019.8778484.

[13] Leon Freris and David Infield. 2008. "*Renewable Energy in Power Systems"* United Kingdom: John Wiley & Sons Ltd.

[14] Lyden, S., and M. E. Haque. 2015. "Maximum power point tracking techniques for photovoltaic systems: A comprehensive review and comparative analysis," *Renewable and Sustainable Energy Reviews 52:1504-1518*.

[15] Maissa Farhat, Oscar Barambones, and Lassaad Sbita. 2015. "Real-Time efficiency boosting for PV systems using MPPT based on sliding mode." *Energy Procedia*, 75: 361–366.

[16] Maissa Farhat, Oscar Barambones, and Lassaad Sbita. 2016. "A new maximum power point method based on a sliding mode approach for solar energy harvesting." *Applied Energy* [Online]. Available: http://dx.doi.org/10.1016/j.apenergy.2016.03.055

[17] Meenal Jain, and NilanshuRamteke. 2013. Modeling and simulation of solar photovoltic module using matlab/Simulink. *IOSR Journal of Computer Engineering*. [Online]. *15(5)*: 27–34. Available: http:// www.iosrjournals.org

[18] Saravanan, S., and Ramesh Babu, N. 2016. "Maximum power point tracking algorithms for photovoltaic system – A review," *Renewable and Sustainable Energy Reviews, 57: 192-204*.

[19] Suneel Deambi. 2011. "*Solar PV Power - A Global Perspective*." New Delhi, India: The Energy and Resources Institute.

[20] Tamal Biswas, G K Panda, and P K Saha. 2015. "Design of boost converter of sliding mode control powered by PV array." *International Journal of Advanced Research in Electrical, Electronics and Instrumentation Engineering* 4(5): 4577–4583.

[21] YoashLevron, and Doron Shmilovitz. 2013. "Maximum power point tracking employing sliding mode control," *IEEE Trans. Circuits and Systems-I: Regular papers 60(3):* 724–732.

[22] Zahra Mirbagheri, S., Saad Mekhilef, and S. Mohsen Mirhassani. 2013. "MPPT with Inc.Cond method using conventional interleaved boost converter," *Energy Procedia*, 42: 24–32.